

# HIGH LUMINOSITY 100 TeV PROTON-ANTIPROTON COLLIDER

S. J. Oliveros\*, J. G. Acosta, L. M. Cremaldi, T. L. Hart, D. J. Summers  
University of Mississippi - Oxford, University, MS 38677, USA

## Abstract

The energy scale for new physics is known to be in the multi-TeV range, signaling the potential need for a collider beyond the LHC. A  $10^{34} \text{ cm}^{-2} \text{ s}^{-1}$  luminosity 100 TeV proton-antiproton collider is explored. Prior engineering studies for 233 and 270 km circumference tunnels were done for Illinois dolomite and Texas chalk signaling manageable tunneling costs. At a  $p\bar{p}$  the cross section for high mass states is of order  $10\times$  higher with antiproton collisions, where antiquarks are directly present rather than relying on gluon splitting. The higher cross sections reduce the synchrotron radiation in superconducting magnets, because lower beam currents can produce the same rare event rates. In our design the increased momentum acceptance ( $11 \pm 2.6 \text{ GeV}/c$ ) in a Fermilab-like antiproton source is used with septa to collect  $12\times$  more antiprotons in 12 channels. For stochastic cooling, 12 cooling systems would be used, each with one debuncher/momentum equalizer ring and two accumulator rings. One electron cooling ring would follow. Finally antiprotons would be recycled during runs without leaving the collider ring, by joining them to new bunches with synchrotron damping.

## PROTON ANTIPROTON COLLIDER REMARKS

Physics beyond the standard model will motivate searches for new high mass states at present and future colliders for years to come. It is readily understood that direct  $q\bar{q}$  annihilation processes make a significant contribution to the production cross section for high mass states, in addition to gluon splitting present in both  $p\bar{p}$  and  $pp$  collisions. The presence of the anti-quark in the  $\bar{p}$  gives a significant advantage to  $p\bar{p}$  colliders for production of high mass states near threshold [1–4].

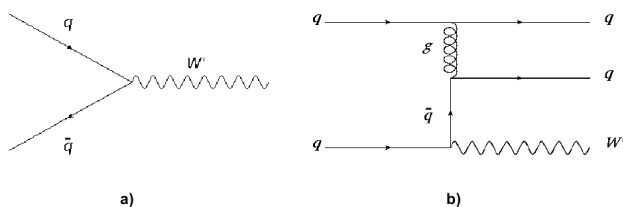


Figure 1: Feynman diagrams for  $W'$  production in (a)  $q\bar{q}$  collision, and (b)  $qq$  collision ( $t$  channel). The two final state quarks cross in the  $u$  channel, which is not shown.

Figure 1 shows the Feynman diagram for  $W'$  production from  $q\bar{q}$  and  $qq$  collision. Using the event generator, Madgraph [5], the  $W'$  cross section is obtained for different  $W'$

\* solivero@go.olemiss.edu

masses using proton-proton and proton-antiproton collisions at a center of mass energy of 100 TeV. The results are shown in the Fig. 2. As the mass increases the  $W'$  cross section obtained with  $p\bar{p}$  collisions is greater compared to  $pp$  collisions, becoming approximately 10 times larger at higher masses.

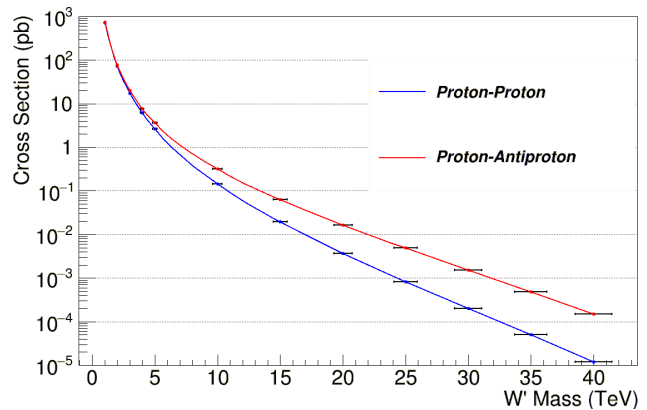


Figure 2:  $W'$  boson production cross section as a function of the mass for  $pp$  and  $p\bar{p}$  collisions with a  $E_{cm} = 100 \text{ TeV}$ .

Synchrotron radiation (SR) effects, growing as  $E^4/\rho^2$ , may become a serious problem in a collider's superconducting magnets and vacuum systems, but less so in  $p\bar{p}$  designs. See the recent design of a 100 km high energy (100 TeV)  $pp$  collider (FCC-hh) [6]. With higher cross sections available at a  $p\bar{p}$  collider it can be run at lower luminosities, with less SR effect, and even less detector pileup. Scaling to a 200 km  $p\bar{p}$  ring, the SR is reduced from 35 W/m [6] to 1.75 W/m.

## OBTAINING HIGH LUMINOSITY

An important goal in designing the 100 TeV  $p\bar{p}$  collider will be achieving a luminosity of  $10^{34} \text{ cm}^{-2} \text{ s}^{-1}$ . As a starting point, taking as reference the Tevatron collider, the gain in luminosity for the 100 TeV  $p\bar{p}$  collider, for which the beam energy is 50 TeV, the ring circumference is 200 km, and  $\beta^* = 14 \text{ cm}$  (half of the Tevatron), the luminosity can

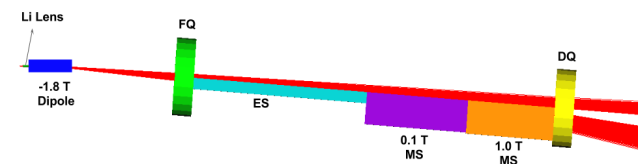


Figure 3: Configuration to divide the beam into two parts. An initial beam with momentum acceptance  $p = 11.0 \text{ GeV}/c \pm 24\%$  is collected by the Li lens and dispersed by a magnetic dipole to be then divided by an electrostatic septa ES and two magnetic dipoles MS.

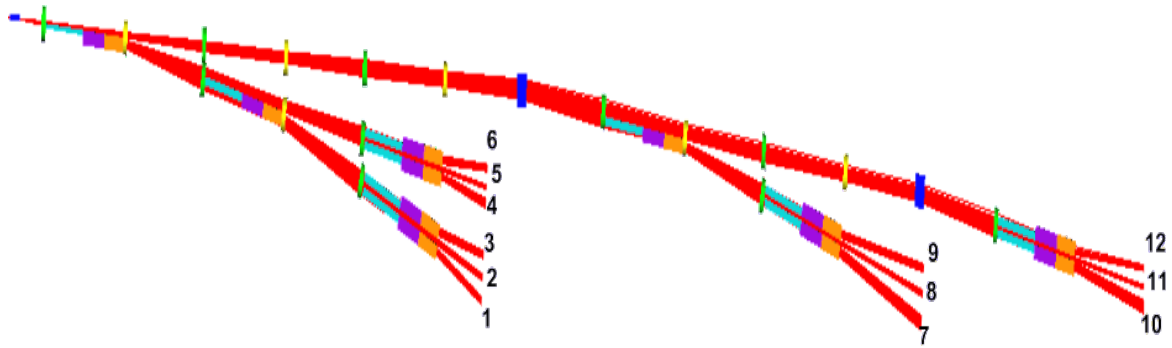


Figure 4: An initial beam with momentum acceptance  $p = 11.0 \text{ GeV}/c \pm 24\%$  is divided to get finally twelve beam with momentum acceptance of  $\pm 2\%$ .

be scaled as,

$$L_{\text{scaled}} = E_{\text{increased}} \times f_{\text{decreased}} \times \beta_{\text{factor}}^* \times L_{\text{current}}$$

$$= \frac{50 \text{ TeV}}{0.98 \text{ TeV}} \times \frac{6.28 \text{ km}}{200 \text{ km}} \times 2 \times (3.4 \times 10^{32} \text{ cm}^{-2} \text{ s}^{-1})$$

$$= 1.1 \times 10^{33} \text{ cm}^{-2} \text{ s}^{-1}$$

Thus, with 10x more bunches a luminosity of  $10^{34}$  is achieved. The antiproton burn rate for a 100 TeV  $p\bar{p}$  collider, with total cross section  $\sigma = 150 \text{ mbarn}$  [7] and  $L = 10^{34} \text{ cm}^{-2} \text{ s}^{-1}$  is  $\sigma L$  or  $540 \times 10^{10} \bar{p}/\text{hr}$ .

The Fermilab Debuncher cooled  $40 \times 10^{10} \bar{p}/\text{hr}$ , thus the number of antiprotons needed are roughly 12 times more. In the Fermilab antiproton source a large fraction of antiprotons were rejected because of the momentum acceptance, which was  $8.9 \text{ GeV}/c \pm 2\%$ . We thus focus on collecting more of these antiprotons, specifically  $\pm 24\%$ . To collect more antiprotons a Fermilab-like target station would be used.

Figure 3 presents the simulation of the basic cell to divide the initial dispersed beam into two using G4beamline [8]. An initial beam enters the Li lens and then is spread by a  $-1.8 \text{ T}$  dipole. An electrostatic septa (ES) divides the beam. Next to the electrostatic septa a  $0.1 \text{ T}$  magnetic septa (MS) is placed to increase the beam separation. A  $3.0 \text{ m}$  long magnetic septa,  $1.0 \text{ T}$ , is placed next to the  $0.1 \text{ T}$  dipole to allow a greater separation between the divided beams. To transport the beam focusing and defocusing quadrupoles are used. The process is repeated to separate the deflected beam into two again, obtaining two beams, and finally each of these beams is separated into three to get the first six beams (Fig. 4). To obtain the next six beams, the initial half beam, which is was not deflected is transported to be dispersed using a second  $-1.8 \text{ T}$  dipole. Then, the same configuration is used to obtain the others six beams. At the end 12 beams are obtained as is shown in Fig. 4.

At Fermilab [9–15], antiprotons were stochastically pre-cooled in the Debuncher ring in  $2.2 \text{ s}$ , with transverse emittance reduction from  $300$  to  $30 \mu\text{m}$ , then sent them to the Accumulator ring to be stochastically cooled and stacked. There, the transverse emittance was reduced from  $30$  to  $3 \mu\text{m}$ . The stochastic cooling time scales as the number of particles.

Thus, to cool 12x more antiprotons, 12 independent cooling systems would be implemented as shown in Fig. 5.

Each debuncher ring phase rotates the beam to lower the momentum spread and also ramps the beam central momenta up or down to  $8.9 \text{ GeV}/c$ , thus the central momenta of all 12 channels would be equalized. The debuncher would alternately feed two accumulator rings. This doubles the time in the accumulator ring deposition orbit for more cooling and reduces required stack sizes. The single Accumulator ring and reduces required stack sizes. The single Accumulator ring follows the stochastic cooling. Electrons can cool large numbers of low emittance antiprotons in one ring [17]. Electron cooling increases as the inverse square of the relativistic  $\gamma$  factor and linearly with the ring fraction  $\eta$  occupied by electrons. Lowering  $\gamma$  by a factor of 3 and increasing  $\eta$  by 10 would increase cooling by 90.

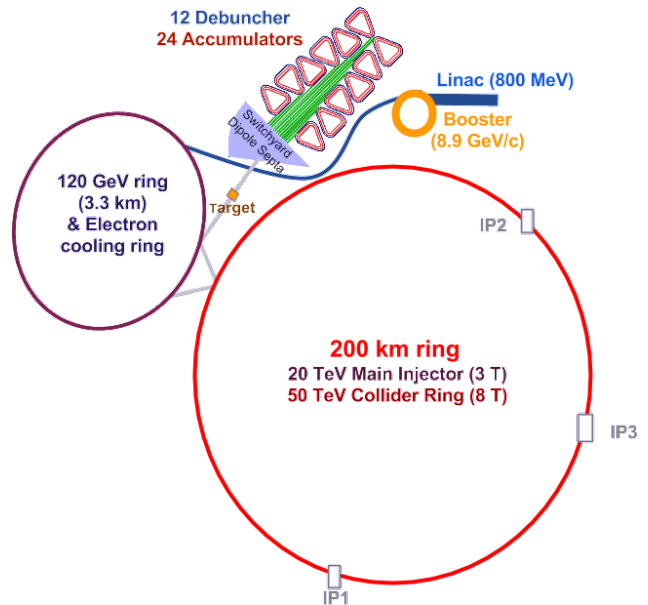


Figure 5: 100 TeV proton-antiproton collider.

Finally antiprotons would be recycled during runs without leaving the collider ring, by joining them to new bunches with snap bunch coalescence and synchrotron damping. The

longitudinal damping time is 2 hours. This effectively increases antiproton production by a factor of two and allows running a second detector at  $L = 10^{34} \text{ cm}^{-2} \text{ s}^{-1}$ .

In addition of getting 10 times as many antiproton bunches to get the desired luminosity,  $\beta^*$  is reduced 28 to 14 cm. The Tevatron used NbTi final focus quadrupole triplets, which could be replaced with Nb<sub>3</sub>Sn quadrupoles, that can reach 13 T fields [18]. Events from  $p\bar{p}$  collisions are more central than  $pp$  collisions allowing a shorter detector with quadrupoles closer to the IP. The Tevatron triplet quadrupole system is taken as a reference to determine the new parameters for a 100 TeV collision energy. This is simulated using Mad-X [19], where the  $\beta^*$  value is fixed and the quadrupole lengths are varied in order to get  $\beta_{x,\max} = \beta_{y,\max}$  in the beta functions plot (Fig. 6). In order to keep the same distance from the interaction point to the quadrupole Q1 ( $L^*$ ) and  $\beta^* = 14 \text{ cm}$ , the quadrupole length ( $l$ ), the separation between the quadrupoles ( $a$ ) are increased by a factor of 5. Figure 6 shows the inner triplet quadrupole system scaled, where  $\beta_{x,\max} = \beta_{y,\max} = 27 \text{ km}$ . Also, to get that optimization the field gradients of the quadrupoles are fixed to be 605 T/m for Q1 and Q3, and 354 T/m for Q2.

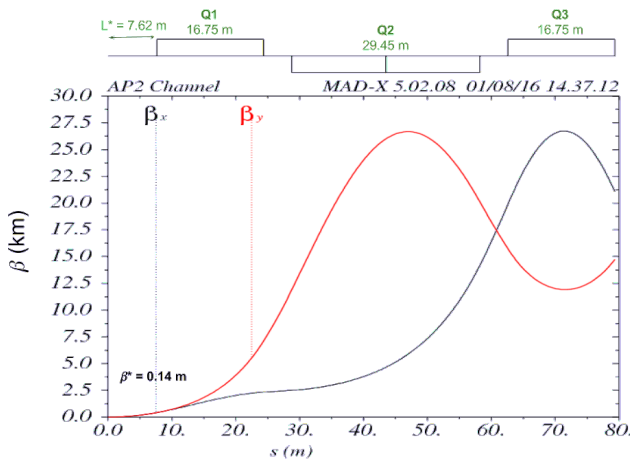


Figure 6: Beta functions plots for the 100 TeV  $p\bar{p}$  collider interaction region.

Using the  $\beta_{\max}$  value, a maximum beam size of 1.1 mm is obtained. The quadrupoles field aperture should be around  $10 \sigma_{\max}$  [20] to be large enough for the beam, and a factor of 2 for field quality could be added, to get finally a 40 mm aperture. Reducing  $\beta^*$  and bunch length by a factor of two allows one to double the number of bunches and halve pileup, while keeping the luminosity constant.

## COLLIDER PARAMETERS

For the construction of the 100 TeV  $p\bar{p}$  collider, two possible sites are considered: Fermilab [21] and Dallas, Texas [22]. Fermilab has the advantage of existing infrastructure and Texas has the advantage of lower tunneling costs. Figure 5 shows the configuration proposed. Included are an 800 MeV Linac, an 8.9 GeV/c Booster ring, and a 120 GeV ring, which sends protons to the antiproton source.

### 1: Circular and Linear Colliders

#### A01 - Hadron Colliders

For antiproton production, a Fermilab-like antiproton source would be adapted to the new collider with 12 Debuncher and 24 Accumulator rings for stochastic cooling. In the 120 GeV ring, both protons and antiprotons are accelerated to 120 GeV before transfer to the 20 TeV Injector, where once this energy is reached are sent to the 50 TeV collider ring. Both, Injector and Collider ring share the same tunnel. The relatively inexpensive 3 T superferric magnet [23, 24] injector would be built first and used as a collider. The 8 T NbTi magnets would be an upgrade. Collisions would include  $p\bar{p}$ ,  $\bar{p}Pb$ , and asymmetric 20 x 50 TeV  $PbPb$ . Lepton colliders might also share the tunnel [1, 2, 25–32].

The 200 km ring could not be built at CERN due to the difficulty of tunneling under the Jura. Table 1 shows the cost per meter for tunneling with different geography for a 4 m diameter tunnel [33] together with the total cost for a 200 km tunnel. The rock composition in Texas is the fastest to bore, about 45 m/day [34]. Thus a 200 km tunnel in Texas would require 3 years using 4 tunneling machines.

Table 1: Comparison between Tunneling Cost for Three Different Places Considered for a 200 km Collider Ring [33]

|                          | Cost/m   | 200 km tunnel |
|--------------------------|----------|---------------|
| CERN (Molasse/limestone) | \$39,000 | 100 km limit  |
| FERMILAB (Dolomite)      | \$15,000 | \$3 billion   |
| Texas(Chalk/marl)        | \$6,000  | \$1.2 billion |

In a collider the dipole magnets represent a large budget item. A 100 km collider, 100 TeV collider requires expensive Nb<sub>3</sub>Sn 16 T magnets. Three or 4.5 T superferric magnets [23, 24, 35] use about half as much NbTi per Tesla/meter as 8 T  $\cos \theta$  magnets.

## CONCLUSIONS

A high luminosity 100 TeV proton-antiproton collider has advantages as a future collider in order to explore physics beyond the standard model. Among them is the reduction in synchrotron radiation and pileup as compared with a 100 TeV  $pp$  collider, due to higher rare event cross sections. To obtain high luminosity, a Fermilab like antiproton source would be implemented and extended to capture and store 12× more antiprotons, with 36 independent stochastic cooling rings. Finally, two location options are presented to build the proton-antiproton collider. In Texas tunneling is cheaper and at Fermilab the existing facilities would represent an advantage. All ring magnets are made with NbTi.

## ACKNOWLEDGMENTS

Many thanks to DOE, Estia Eichten, Henry Frisch, Peter McIntyre, and Steve Mrenna.

## REFERENCES

- [1] G. T. Lyons III, Master's Thesis, arXiv:1112.1105.
- [2] D. J. Summers *et al.*, *AIP Conf. Proc.* **1507** (2012) 860.

- [3] S. J. Oliveros, in *Proc. COOL2015*, paper TUPF01.
- [4] B. C. Barish *et al.*, SSC-SR-1022 (1986).
- [5] <http://madgraph.hep.uiuc.edu/>;  
J. Alwall *et al.*, *JHEP* **1106** (2011) 128.
- [6] W. Barletta *et al.*, *Nucl. Instrum. Meth.* **A764** (2014) 352.
- [7] W. Barletta *et al.*, arXiv:1310.0290.
- [8] Tom Roberts, G4beamline User Guide 2.16, <http://www.muonsinternal.com/muons3/G4beamline>  
T. J. Roberts *et al.*, in *Proc. EPAC'08*, paper WEPP120.
- [9] J. Peoples, *IEEE Trans. Nucl. Sci.* **30** (1983) 1970.
- [10] Tevatron Design Report, FERMILAB-DESIGN-1984-01.
- [11] R. J. Pasquinelli *et al.*, FERMILAB-CONF-09-126-AD.
- [12] S. Holmes *et al.*, *JINST* **6** (2011) T08001.
- [13] S. Nagaitsev, arXiv:1408.0759.
- [14] C. Rubbia *et al.*, Print-76-0252-HARVARD.
- [15] Simon van der Meer, *Rev. Mod. Phys.* **57** (1985) 689.
- [16] V. Lebedev, in *Proc. COOL'09*, paper MOA1MCCO02 (2009).
- [17] T. Ellison *et al.*, *IEEE Trans. Nucl. Sci.* **30** (1983) 2636.
- [18] P. Ferracin *et al.*, *IEEE Trans. Appl. Supercond.* **24** (2014) 4002306.
- [19] Hans Grote *et al.*, "The MAD-X Program (Methodical Accelerator Design) Version 5.02.08 User's Reference Manual," (2016), <http://madx.web.cern.ch/madx/releases/last-dev/madxguide.pdf>  
W. Herr and F. Schmidt, "A MAD-X Primer," CERN-AB-2004-027-ABP,
- [20] S. Feher and J. Strait, "Estimated Inner Triplet Quadrupole length and Aperture for Really Large Hadron Colliders of  $E_{\text{beam}} = 30, 60, 100$  TeV," SNOWMASS-1996-ACC042.
- [21] G. Ambrosio *et al.*, Fermilab-TM-2149 (2001).
- [22] P. McIntyre *et al.*, arXiv:1402.5973.
- [23] G. W. Foster and V. S. Kashikhin, "Superconducting superferic dipole magnet with cold iron core for the VLHC," *IEEE Trans. Appl. Supercond.* **12** (2002) 111.
- [24] F. R. Huson *et al.*, *IEEE Trans. Nucl. Sci.* **32** (1985) 3462.
- [25] J. Gallardo *et al.*, Snowmass 1996, BNL-52503.
- [26] D. Neuffer, Fermilab -FN- 0319 (1979).
- [27] R. Palmer *et al.*, *AIP Conf. Proc.* **372** (1996) 3.
- [28] R. Palmer *et al.*, *Nucl. Phys. Proc. Suppl.* **51A** (1996) 61.
- [29] C. M. Ankenbrandt *et al.*, *PRSTAB* **2** (1999) 081001.
- [30] R. Palmer *et al.*, *PRSTAB* **8** (2005) 061003.
- [31] M. Chung *et al.*, *Phys. Rev. Lett.* **111** (2013) 184802.
- [32] D. Stratakis and R. Palmer, *PRSTAB* **18** (2015) 031003.
- [33] M. Breidenbach and W. Barletta, "Accelerator Research in the U.S. for High Energy Physics: A biased perspective," ESS-DOC-371 (2015).
- [34] Peter McIntyre *et al.*, "Large Circumference, NbTi Cable-in-Conduit: Industrialization for a 100 TeV Hadron Collider," LPC Meeting on Future 100 TeV Proton Collider, Fermilab, 31 Jan 2014,  
<https://indico.cern.ch/event/294897/>
- [35] P. McIntyre *et al.*, in *Proc. IPAC2015*, paper THPF134.